Journal of Quantitative Spectroscopy & Radiative Transfer 164 (2015) 193–206

Contents lists available at ScienceDirect

Journal of Quantitative Spectroscopy & Radiative Transfer

journal homepage: www.elsevier.com/locate/jqsrt

A comparative study between semi-empirical oscillator strength parametrization and relativistic Hartree–Fock methods for computing the radiative parameters in Zr II spectrum

P. Quinet [a,b,*], S. Bouazza [c], P. Palmeri [a]

[a] Astrophysique et Spectroscopie, Université de Mons, B-7000 Mons, Belgium
[b] IPNAS, Université de Liège, B-4000 Liège, Belgium
[c] LISM, E. A. 4695 Université de Reims-Champagne-Ardenne, UFR SEN, BP 1039, F-51687 Reims Cedex 2, France

ARTICLE INFO

Article history:
Received 15 May 2015
Received in revised form
6 June 2015
Accepted 9 June 2015
Available online 23 June 2015

Keywords:
Fine structure
Transition probabilities
Oscillator strengths
Zr II spectrum

ABSTRACT

In the present work, we compare the radiative transition rates computed by two different semi-empirical approaches, based on a parametrization of the oscillator strengths and on a pseudo-relativistic Hartree–Fock model including core-polarization effects, for spectral lines in singly ionized zirconium. A detailed comparison with available experimental results is also reported and an overall good agreement is observed between all sets of data allowing us to provide new reliable oscillator strengths for a large amount of Zr II lines in the wavelength region from 1616 to 14746 Å. Moreover, we give radial integral values of the main atomic transitions deduced in this study: $\langle 4d^25p|r^1|4d^25s\rangle = -3.1522$ (0.0161), $\langle 4d^25p|r^1|4d^3\rangle = 1.7605$ (0.0107), $\langle 4d^25p|r^1|4d^26s\rangle = -1.481$ (0.794) and $\langle 4d^25p|r^1|4d^25d\rangle = 2.289$ (0.014).

1. Introduction

A great deal of experimental work has been done on hyperfine structure and isotope shift of neutral zirconium [1] but only a few measurements concerning these two topics have been achieved so far for Zr II. Regarding Zr II oscillator strength determinations many studies were performed in the past: Corliss and Bozman, using an arc as a light source, were the first to give experimental values of 321 Zr II line oscillator strengths [2]. Two decades later Biémont et al. [3], recurring to lifetimes and branching fractions, reported also 31 line oscillator strength values. Radiative lifetimes of 16 odd levels belonging to the lowest Zr II configurations have been measured by Malcheva et al. [4], using a time-resolved laser induced fluorescence technique with a single-step excitation. This team extended this study since it reported also transition probabilities for 243 transitions combining experimental data with pseudo relativistic Hartree–Fock calculations taking into account core-polarization effects. In the same year Ljung et al. [5] gave oscillator strength values for 263 Zr II lines in the spectral range 2500–5400 Å through two steps: taking advantage of line intensities measured with the Lund Fourier Transform Spectrometer they first derived branching fractions. Afterward they combined the latter with lifetimes obtained by Biémont et al. [3] and deduced oscillator strength values. Theoretically Bogdanovich et al. [6], having recourse to the superposition-of-configuration method, computed oscillator strength values. In the present work, we propose to compare experimental data available in literature to computed values obtained by two semi-empirical

* Corresponding author.
E-mail address: Pascal.Quinet@umons.ac.be (P. Quinet).

http://dx.doi.org/10.1016/j.jqsrt.2015.06.011
0022-4073/

approaches, based on a parameterization of the oscillator strengths and on a pseudo-relativistic Hartree–Fock model including core-polarization effects.

It is worth reminding that the accurate determination of spectroscopic parameters in singly ionized zirconium is of great importance in astrophysics since Zr II lines have been detected in many different types of stars, such as e.g. the Ap stars of the Cr–Eu–Sr subgroup [7,8] or the Bp stars of the Hg–Mn subgroup [9]. Zr has five stable isotopes, namely ^{90}Zr, ^{91}Zr, ^{92}Zr, ^{94}Zr and ^{96}Zr, the first four being only made by the slow neutron capture process (s-process), while the fifth one being made by the rapid process (r-process). There also exist 15 shorter lived isotopes and isomers. Singly ionized zirconium has also been investigated in the context of the Zr abundance in the solar photosphere [3,6]. Moreover, using a limited set of accurate oscillator strengths, Sikström et al. [10] were unable to resolve the anomaly existing in the HgMn star χLupi observed using the Hubble Space Telescope between the zirconium abundance deduced from weak lines of Zr II at optical wavelengths and strong Zr III lines in the UV region in the framework of the Local Thermodynamic Equilibrium (LTE). Although, according to these authors, the difference is probably mainly due to non-LTE or diffusion effects rather than to uncertainties affecting the oscillator strengths, an extended set of reliable transition rates in these ions is highly needed for investigating this problem in a more detailed way.

2. Oscillator strength parametrization method

2.1. Fine structure analysis

For semi-empirical approaches, such as the oscillator strength parametrization method, the determination of very accurate eigenvectors of the two levels of each studied transition is of paramount importance: we have to transform angular coefficients of the transition matrix from SL coupling to intermediate one by means of fine structure (fs) eigenvector amplitudes. Here, L and S represent, respectively, the total angular momentum and the resulting spin quantum numbers for a system of electrons. Sometimes the fine structure analysis is not easy to achieve because there are not enough experimental energy levels to fit in order to determine Slater integrals, spin–orbit constants, configuration–interaction parameters, two-body parameters, etc. Sometimes also the level assignments previously published are questionable.

The Zr II fs was initiated by Kiess [11] and extended by Moore [12]. Meggers, Corliss, and Scribner collected in 1975 the previous data in NIST compilation [13]. Some years ago we studied the three lowest even-parity configuration fs, gathering 37 levels in the model space $(4d+5s)^3$ [14]. This time we consider a bigger set of configurations: $4d^25s$, $4d^3$, $4d5s^2$, $4d^26s$, $4d^25d$, $4d5p^2$ and $4d5d^2$.

Table 1
Fine structure parameter values adopted for even-parity configurations in the oscillator strength parametrization method. All values are given in cm^{-1}.

Config.	$4d^25s$	$4d^3$	$4d^26s$	$4d^25d$	$4d5s^2$	$4d5p^2$	$4d5d^2$
E_{av}	7756 (12)	12,071 (16)	69,620 (18)	73,107 (114)	15,322 (23)	81,872	105,900
$F^2(4d,4d)$	35,143 (40)	33,385 (41)	37,080 (105)	37,080			
$F^4(4d,4d)$	20,572 (50)	20,345 (59)	22,969 (430)	22,556			
$F^2(5p,5p)$						19,224	
$F^4(5p,5p)$							
$G^0(4d,5d)$				2553			2748
$G^1(4d,5p)$						6448	
$G^2(4d,5s)$	11,929 (29)		2644 (34)				
$G^2(4d,5d)$				2100			2450
$G^3(4d,5p)$						5142	
$F^2(4d,5d)$				5142			6437
$F^4(4d,5d)$				1501			2894
$F^2(4d,5p)$						13,523	
$F^2(4d,5d)$							12,720
$F^2(5d,5d)$							8640
ζ_{4d}	372 (8)	325 (9)	376 (6)	376	402	421	445
ζ_{5d}				36			50
ζ_{5p}						838	
Ts(4d,4d,ns)	32		32				
α	9 (1)	9 (1)	9 (1)	9 (1)			
β	−99 (13)	−99 (13)	−99 (13)	−99 (13)			
CI	D^0	E^2	D^2	R^2	R^4		
$4d^25s$–$4d^3$				−14,681 (20)			
$4d^25s$–$4d^26s$	480 (48)	4800 (279)					
$4d^25s$–$4d^25d$		−700	2100				
$4d^25s$–$4d5s^2$				−14,085 (89)			
$4d^3$–$4d^26s$				−3941			
$4d^3$–$4d^25d$	800			5800	3800 (313)		
$4d^3$–$4d5s^2$				15,042 (82)			
$4d^26s$–$4d^25d$		−640	−2100				
$4d^25d$–$4d5s^2$				−1900			

Table 2
Comparison of the observed and calculated even-parity energy levels and g_J-factors (see text). Experimental data are taken from [12].

J	E_{exp} (cm^{-1})	E_{calc} (cm^{-1})	g_{exp}	g_{calc}	1st LS component (%)	2nd LS component (%)
1/2	5724.38	5716.46	0.690	0.683	59.2 4d^3 ^{2}P	39.7 4d^2(^{3}P)5s ^{2}P
	7512.67	7513.99	2.656	2.666	99.6 4d^2(^{3}P)5s ^{4}P	0.2 4d^2(^{1}S)5s ^{2}S
	9553.10	9564.26	2.649	2.656	98.8 4d^3 ^{4}P	0.5 4d^2(^{3}P)5s ^{2}P
	19,613.54	19,618.41	0.514	0.674	57.5 4d^2(^{3}P)5s ^{2}P	39.5 4d^3 ^{2}P
	25,201.57	25,198.77	1.990	1.996	98.5 4d^2(^{1}S)5s ^{2}S	0.7 4d5p^2 ^{2}S
3/2	0.00	−13.44	0.398	0.403	98.9 4d^2(^{3}F)5s ^{4}F	0.8 4d^2(^{1}D)5s ^{2}D
	2572.21	2574.73	0.413	0.417	95.3 4d^3 ^{4}F	1.6 4d^2(^{1}D)5s ^{2}D
	4248.30	4214.70	0.812	0.813	46.4 4d^2(^{1}D)5s ^{2}D	20.9 4d5s^2 ^{2}D
	6111.70	6118.69	1.304	1.310	55.2 4d^3 ^{2}P	36.0 4d^2(^{3}P)5s ^{2}P
	7736.02	7739.00	1.720	1.730	99.1 4d^2(^{3}P)5s ^{4}P	0.3 4d^3 ^{2}P
	9742.80	9754.78	1.721	1.727	97.6 4d^3 ^{4}P	1.3 4d^2(^{3}P)5s ^{2}P
	13,428.50	13,440.42	0.800	0.801	65.7 4d5s^2 ^{2}D	22.9 4d^2(^{1}D)5s ^{2}D
	14,298.64	14,321.07	0.807	0.805	56.2 4d^3 ^{2}D	23.8 4d^2(^{1}D)5s ^{2}D
	20,080.30	20,067.39	1.326	1.330	57.3 4d^2(^{3}P)5s ^{2}P	39.2 4d^3 ^{2}P
	27,699.96	27,714.01		0.800	69.0 4d^3 ^{2}D	21.0 4d^3 ^{2}D
	63,602.64	63,700.24		0.400	99.2 4d^2(^{3}F)6s ^{4}F	0.4 4d^2(^{3}F)5d ^{4}F
5/2	314.67	308.52	1.023	1.029	99.1 4d^2(^{3}F)5s ^{4}F	0.4 4d^2(^{1}D)5s ^{2}D
	2895.05	2904.11	1.025	1.032	98.1 4d^3 ^{4}F	0.7 4d^2(^{1}D)5s ^{2}D
	4505.50	4542.10	1.172	1.177	51.5 4d^2(^{1}D)5s ^{2}D	17.7 4d5s^2 ^{2}D
	5752.92	5776.04	0.883	0.884	84.2 4d^2(^{3}F)5s ^{2}F	6.9 4d^3 ^{2}F
	8058.16	8066.43	1.585	1.594	98.2 4d^2(^{3}P)5s ^{4}P	0.7 4d5s^2 ^{2}D
	9968.65	9963.76	1.593	1.600	99.2 4d^3 ^{4}P	0.3 4d5p^2 ^{4}P
	14,162.90	14,155.23	1.209	1.201	68.1 4d5s^2 ^{2}D	19.5 4d^2(^{1}D)5s ^{2}D
	14,733.37	14,731.69	1.188	1.201	60.2 4d^3 ^{2}D	23.0 4d^2(^{1}D)5s ^{2}D
	19,514.84	19,528.65	0.855	0.859	91.1 4d^3 ^{2}F	7.2 4d^2(^{3}F)5s ^{2}F
	27,640.60	27,644.83		1.200	70.9 4d^3 ^{2}D	17.4 4d^3 ^{2}D
	63,868.45	63,935.16	1.110	1.026	97.5 4d^2(^{3}F)6s ^{4}F	1.9 4d^2(^{3}F)6s ^{2}F
7/2	763.44	762.53	1.235	1.238	99.7 4d^2(^{3}F)5s ^{4}F	0.3 4d^2(^{3}F)5s ^{2}F
	3299.64	3310.50	1.227	1.238	99.6 4d^3 ^{4}F	0.2 4d^3 ^{2}G
	6467.61	6456.85	1.144	1.142	89.3 4d^2(^{3}F)5s ^{2}F	8.5 4d^3 ^{2}F
	7837.74	7848.21	0.887	0.891	72.9 4d^3 ^{2}G	26.3 4d^2(^{1}G)5s ^{2}G
	14,059.76	14,049.09	0.890	0.889	72.6 4d^2(^{1}G)5s ^{2}G	26.4 4d^3 ^{2}G
	19,433.24	19,449.07	1.153	1.143	90.4 4d^3 ^{2}F	8.3 4d^2(^{3}F)5s ^{2}F
	64,368.28	64,301.64	1.205	1.237	98.1 4d^2(^{3}F)6s ^{4}F	1.5 4d^2(^{3}F)6s ^{2}F
9/2	1322.91	1325.95	1.324	1.334	99.8 4d^2(^{3}F)5s ^{4}F	0.1 4d^2(^{1}G)5s ^{2}G
	3757.66	3763.88	1.326	1.332	98.8 4d^3 ^{4}F	0.9 4d^3 ^{2}G
	8152.80	8151.58	1.107	1.111	68.8 4d^3 ^{2}G	28.7 4d^2(^{1}G)5s ^{2}G
	11,984.46	12,010.43	0.910	0.915	96.8 4d^3 ^{2}H	2.9 4d^2(^{1}G)5s ^{2}G
	14,190.45	14,216.16	1.103	1.108	67.6 4d^2(^{1}G)5s ^{2}G	29.8 4d^3 ^{2}G
	64,901.71	64,782.85	1.274	1.334	99.6 4d^3 ^{4}F	0.2 4d^2(^{3}F)6s ^{4}F
11/2	12,359.66	12,356.23	1.091	1.091	99.8 4d^3 ^{2}H	0.1 4d^2(^{3}F)5d ^{2}H

The fs least square fitting procedure has been carried out over all even-parity levels available in literature up to 66,000 cm^{-1}. With 42 parameters, 12 of which were treated as free, an excellent fit has been achieved. Table 1 contains the values of fs radial parameters obtained thanks to the fitting procedure. When fs parameters are given without uncertainties this means that these parameters were given simply *ab initio* values or were deduced by links with other parameters thanks to *ab initio* ratio of the corresponding parameters. Let us add that values of some parameters, although predicted by theory but expected to be small in this study, were fixed to zero and then are not listed in this table. In Table 2 the experimental energy levels, calculated eigenvalues, resulting *LS*-percentage of first and second components of the wave functions, and the corresponding *LS*-term designations are given. In this table experimental Landé g_J-factors are compared to those deduced from the eigenvector compositions. In this study we confirm what we previously mentioned: the two doublets b ^{2}D et c ^{2}D are inverted, i.e. b ^{2}D belongs rather to 4d5s^2 instead of 4d^3 and c ^{2}D belongs rather to 4d^3 instead of 4d5s^2.

Usually odd-parity level fs analysis is rather more difficult to perform than even-parity level one, due to presence of very complex mixing concerning odd-parity configurations: in this case the levels of 4d5s5p overlap levels from both the 4d^{2}5p and 5s^{2}5p configurations. Furthermore, Zr II odd-parity level fs has never been experimentally studied during these last 6 decades. We decided to fit 65 levels, whose energies do not exceed 60,000 cm^{-1} for many reasons: we planned in this work to study oscillator strengths of transitions linking mainly levels of the two lowest odd configurations even if for determination of eigenvector level compositions we need to consider a set of the 6 lowest configurations. Moreover, there are experimental Landé-factor values only up to 55,000 cm^{-1} for each J-matrix. In absence of g_J value it is more difficult to assign levels. At least if there are hyperfine structure or/and isotope shift data we can compensate

Table 3
Fine structure parameter values adopted for odd-parity configurations in the oscillator strength parametrization method. All values are given in cm^{-1}.

Config.	$4d^25p$	4d5s5p	$5s^25p$	$4d^26p$	$5s^26p$
E_{av}	36,801 (19)	44,245 (35)	61,379 (320)	66,075	85,000
F^2(4d,4d)	36,142 (114)			35,000	
F^4(4d,4d)	22,128 (165)			23,000	
G^1(4d,np)	6694 (47)	8660 (233)		1280	
G^2(4d,5s)		10,906 (370)			
G^3(4d,np)	2677 (83)	2048 (450)		1180	
G^1(5s,5p)		22,108 (345)			
F^2(4d,np)	10,643 (92)	15,606 (134)		3340	
ζ_{4d}	379 (21)	435 (31)		375	
ζ_{np}	890 (52)	944 (63)	1065 (272)	230	254
α	38	38			
β	−8	−8			
CI	D^2	R^2	R^4	E^1	
$4d^25p$–4d5s5p	−8290 (74)	−15,751 (110)		−9234 (68)	
$4d^25p$–$5s^25p$		10,879 (131)			
$4d^25p$–$4d^26p$	4556			1400	
4d5s5p–$5s^25p$	−9866 (180)			−15,120 (138)	
4d5s5p–$4d^26p$	−1866			−2862	

these deficiencies. In this study the following configurations are involved: $4d^25p$, 4d5s5p, $5s^25p$, $4d^26p$ and $5s^26p$. We give in Table 3 the fs parameters for this set. In Table 4 we give for the first time calculated eigenvalues, resulting *LS*-percentage of first and second components of the wave functions, the corresponding *LS*-term designations and calculated Landé g_J-factors, recurring to the level eigenvector composition.

2.2. Oscillator strength and transition probability determination

As in case of our previous study devoted to Hf II [15] we looked first into electric dipole transitions. We had recourse to a semi-empirical method for parameterization of oscillator strengths. The complete details of this method were described for the first time in a paper presented by Ruczkowski et al. [16]; nevertheless let us mention once more that we transformed angular coefficients of the transition matrix from SL coupling to intermediate one, using the determined fine structure eigenvector amplitudes.

For the electric dipole transitions, the weighted oscillator strength *gf* is related to the line strength **S** [17]:

$$gf = 8\pi^2 mca_0^2\frac{\sigma}{3h}\mathbf{S} = 303.76\times10^{-8}\sigma\mathbf{S}, \tag{1}$$

where a_0 is the Bohr radius, $\sigma = |E(\gamma)-E(\gamma')|/hc$ and h is Planck's constant. Let us point out that $E(\gamma)$ is the energy of the initial state. The quantities with primes refer to the final state.

The electric dipole line strength is defined by

$$\mathbf{S} = |<\gamma J\,||\mathbf{P^1}||\gamma' J'>|^2, \tag{2}$$

The tensorial operator $\mathbf{P^1}$ in the reduced matrix element represents the electric dipole moment.

For multiconfiguration system, the wavefunctions $|\gamma J>$ and $|\gamma' J'>$ are expanded in terms of a set of basis functions $|\psi SLJ>$ and $|\psi' S'L'J'>$, respectively:

$$|\gamma J> = \sum_i c_i|\psi SLJ>,\ |\gamma' J'> = \sum_j c_j'|\psi' S'L'J'> \tag{3}$$

The square root of the line strength may be written in the following form:

$$S^{1/2}_{\gamma\gamma'} = \sum_i\sum_j c_i c_j' <\psi SLJ||\mathbf{P^1}||\psi' S'L'J'> \tag{4}$$

From Eqs. (2) and (4), we can express the *gf*-values as a linear combination:

$$(gf)^{1/2} = \sum\nolimits_{nl,n'l'}(303.76\sigma\times10^{-8})^{1/2} \times\sum_i\sum_j c_i c_j' <\psi SLJ||\mathbf{P^1}||\psi' S'L'J'>, \tag{5}$$

and the sum is over all possible transitions (ns↔n′p, nd↔n′p) and presently studied for odd-parity levels.

The weighted transition probability is

$$gA = (2j'+1)A = 64\pi^4 e^2 a_0^2\sigma^3\mathbf{S}/3h = 2.0261\times10^{-6}\sigma^3\mathbf{S} \tag{6}$$

where σ is given in cm^{-1} and **S** in atomic units of $e^2a_0^2$

Using Eqs. (1) and (6) one obtains in s^{-1}:

$$gA = 0.66702\sigma^2 gf \tag{7}$$

As regards determination of radial transition integrals one can notice that our method differs totally from the Kurucz's one. Kurucz [19] uses Thomas–Fermi–Dirac method to compute transition integral values. In many approximate methods, the statistical one founded by Thomas and Fermi and later modified by Dirac is sufficient to treat problems concerning bulky properties of the atom and is very useful, especially for the atoms or ions with large atomic number. This is unfortunately not the case of Zr II which is a medium Z (=40) element.

Here we have recurring to Eq. (5) where beforehand we computed angular part of the electric dipole moment with

Table 4
Comparison of the observed and calculated odd-parity energy levels and g_J-factors (see text). Experimental data are taken from [12].

J	E_{exp} (cm^{-1})	E_{calc} (cm^{-1})	g_{exp}	g_{calc}	1st LS component (%)	2nd LS component (%)
1/2	31,981.25	32,045.20	0.016	0.009	86.3 4d^2(^{3}F)5p ^{4}D	11.6 4d5s(^{3}D)5p ^{4}D
	34,810.03	34,610.09	1.956	1.973	91.7 4d^2(^{3}P)5p ^{2}S	3.6 4d^2(^{3}P)5p ^{4}P
	36,196.57	36,102.46	0.610	0.577	60.9 4d^2(^{1}D)5p ^{2}P	18.1 4d^2(^{3}P)5p ^{4}D
	36,237.04	36,224.01	0.144	0.177	62.4 4d^2(^{3}P)5p ^{4}D	16.8 4d^2(^{1}D)5p ^{2}P
	38,063.40	37,933.73	2.448	2.550	74.7 4d^2(^{3}P)5p ^{4}P	16.8 4d5s(^{3}D)5p ^{4}P
	38,934.37	38,874.75	0.055	0.062	68.1 4d5s(^{3}D)5p ^{4}D	16.7 4d^2(^{3}P)5p ^{4}D
	40,727.26	41,017.15	0.677	0.664	55.2 4d^2(^{3}P)5p ^{2}P	12.2 4d5s(^{3}D)5p ^{2}P
	42,789.24	42,884.67	2.632	2.636	81.5 4d5s(^{3}D)5p ^{4}P	16.7 4d^2(^{3}P)5p ^{4}P
	45,944.00	45,750.80	0.724	0.685	51.3 4d5s(^{1}D)5p ^{2}P	23.0 4d^2(^{3}P)5p ^{2}P
	52,585.80	52,558.97	0.659	0.667	43.4 4d^2(^{1}S)5p ^{2}P	30.8 4d5s(^{1}D)5p ^{2}P
3/2	29,777.60	29,719.29	0.700	0.644	43.3 4d^2(^{3}F)5p ^{2}D	41.1 4d^2(^{3}F)5p ^{4}F
	30,435.38	30,476.14	0.589	0.607	46.4 4d^2(^{3}F)5p ^{4}F	19.7 4d^2(^{3}F)5p ^{2}D
	32,256.71	32,278.26	1.166	1.161	78.1 4d^2(^{3}F)5p ^{4}D	9.7 4d5s(^{3}D)5p ^{4}D
	32,983.73	32,983.53	0.810	0.826	28.3 4d5s(^{3}D)5p ^{2}D	26.5 4d^2(^{1}D)5p ^{2}D
	35,914.81	35,703.26	1.340	1.307	75.0 4d^2(^{1}D)5p ^{2}P	5.9 4d5s(^{1}D)5p ^{2}P
	36,638.50	36,428.56	1.038	0.980	59.6 4d^2(^{3}P)5p ^{4}D	26.7 4d5s(^{3}D)5p ^{4}F
	36,451.79	36,539.13	0.579	0.641	66.3 4d5s(^{3}D)5p ^{4}F	21.5 4d^2(^{3}P)5p ^{4}D
	37,681.75	37,868.73	1.908	1.918	75.1 4d^2(^{3}P)5p ^{4}S	16.4 4d^2(^{3}P)5p ^{4}P
	38,133.50	38,405.32	1.734	1.756	58.9 4d^2(^{3}P)5p ^{4}P	20.3 4d^2(^{3}P)5p ^{4}S
	39,192.35	39,170.63	1.209	1.219	67.3 4d5s(^{3}D)5p ^{4}D	15.7 4d^2(^{3}P)5p ^{4}D
	41,337.36	41,255.82	1.326	1.325	65.2 4d^2(^{3}P)5p ^{2}P	12.2 4d5s(^{3}D)5p ^{2}P
	41,467.72	41,586.48	0.821	0.829	70.2 4d^2(^{3}P)5p ^{2}D	14.2 4d5s(^{1}D)5p ^{2}D
	42,893.54	42,889.78	1.710	1.707	76.3 4d5s(^{3}D)5p ^{4}P	17.8 4d^2(^{3}P)5p ^{4}P
	45,054.87	45,171.90	0.870	0.851	42.5 4d^2(^{1}D)5p ^{2}D	29.6 4d5s(^{3}D)5p ^{2}D
	45,568.21	45,570.44	1.140	1.300	53.0 4d5s(^{1}D)5p ^{2}P	11.1 4d^2(^{3}P)5p ^{2}P
	52,876.80	52,864.10	1.318	1.326	45.6 4d5s(^{1}S)5p ^{2}P	21.9 4d5s(^{1}D)5p ^{2}P
	55,835.53	55,757.03		0.808	70.8 4d5s(^{3}D)5p ^{2}D	9.9 4d^2(^{3}F)6p ^{2}D
5/2	27,983.83	28,053.13	0.664	0.660	71.4 4d^2(^{3}F)5p ^{4}G	16.7 4d^2(^{3}F)5p ^{2}F
	29,504.97	29,609.64	0.841	0.879	31.3 4d^2(^{3}F)5p ^{2}F	24.7 4d^2(^{3}F)5p ^{4}G
	30,551.48	30,511.99	1.046	1.035	76.1 4d^2(^{3}F)5p ^{4}F	8.6 4d^2(^{3}F)5p ^{2}D
	31,160.04	31,189.12	1.117	1.110	31.5 4d^2(^{3}F)5p ^{2}D	13.9 4d^2(^{3}F)5p ^{4}F
	32,614.71	32,588.06	1.342	1.343	75.7 4d^2(^{3}F)5p ^{4}D	8.7 4d5s(^{3}D)5p ^{4}D
	33,419.45	33,527.50	1.195	1.202	30.6 4d5s(^{3}D)5p ^{2}D	30.2 4d^2(^{3}F)5p ^{2}D
	36,869.00	36,774.69	1.091	1.034	28.1 4d^2(^{1}D)5p ^{2}F	20.9 4d^2(^{3}P)5p ^{4}D
	37,171.22	37,032.39	1.140	1.229	58.0 4d^2(^{3}P)5p ^{4}D	14.0 4d^2(^{1}D)5p ^{2}F
	37,346.31	37,183.96	0.975	1.003	73.0 4d5s(^{3}D)5p ^{4}F	11.5 4d^2(^{1}D)5p ^{2}F
	38,482.64	38,482.48	1.606	1.580	73.1 4d^2(^{3}P)5p ^{4}P	19.8 4d5s(^{3}D)5p ^{4}P
	39,640.08	39,668.16	1.370	1.379	67.1 4d5s(^{3}D)5p ^{4}D	16.9 4d^2(^{3}P)5p ^{4}D
	41,676.82	41,459.74	1.184	1.208	70.0 4d^2(^{3}P)5p ^{2}D	10.5 4d5s(^{1}D)5p ^{2}D
	42,860.72	42,890.47	0.887	0.881	77.1 4d^2(^{1}G)5p ^{2}F	10.0 4d5s(^{3}D)5p ^{2}F
	43,202.45	43,098.77	1.561	1.551	69.3 4d5s(^{3}D)5p ^{4}P	19.5 4d^2(^{3}P)5p ^{4}P
	45,186.05	45,317.18	1.226	1.215	45.8 4d^2(^{1}D)5p ^{2}D	34.4 4d5s(^{3}D)5p ^{2}D
	47,881.88	47,864.81	0.871	0.866	74.9 4d5s(1D)5p ^{2}F	13.7 4d^2(^{1}D)5p ^{2}F
	56,569.44	56,554.08	1.160	1.147	61.7 4d5s(^{3}D)5p ^{2}D	12.7 4d5s(^{3}D)5p ^{2}F
	57,062.00	57,120.42		0.910	66.2 4d5s(^{3}D)5p ^{2}F	11.4 4d5s(^{3}D)5p ^{2}D
7/2	28,909.04	28,940.20	0.998	1.002	89.2 4d^2(^{3}F)5p ^{4}G	6.4 4d^2(^{3}F)5p ^{2}F
	30,561.75	30,641.59	1.132	1.139	59.5 4d^2(^{3}F)5p ^{2}F	20.6 4d^2(^{1}D)5p ^{2}F
	31,249.28	31,172.67	1.238	1.236	92.4 4d^2(^{3}F)5p ^{4}F	3.7 4d5s(^{3}D)5p ^{4}F
	32,899.46	32,787.32	1.408	1.412	83.8 4d^2(^{3}F)5p ^{4}D	9.2 4d5s(3D)5p ^{4}D
	34,485.42	34,542.74	0.889	0.897	79.8 4d^2(^{3}F)5p ^{2}G	17.5 4d^2(^{1}G)5p ^{2}G
	37,429.76	37,342.00	1.266	1.253	29.0 4d^2(^{3}P)5p ^{4}D	27.5 4d^2(^{1}D)5p ^{2}F
	37,787.59	37,795.89	1.212	1.232	81.9 4d5s(^{3}D)5p ^{4}F	6.5 4d^2(^{1}D)5p ^{2}F
	38,041.49	38,057.21	1.306	1.323	48.0 4d^2(^{3}P)5p ^{4}D	17.5 4d^2(^{1}D)5p ^{2}F
	40,238.55	40,279.73	1.408	1.425	69.1 4d5s(^{3}D)5p ^{4}D	20.3 4d^2(^{3}P)5p ^{4}D
	40,852.74	40,986.54	0.915	0.923	68.9 4d^2(^{1}G)5p ^{2}G	17.8 4d^2(^{3}F)5p ^{2}G
	42,504.11	42,470.33	1.134	1.116	71.8 4d^2(^{1}G)5p ^{2}F	10.0 4d^2(^{1}G)5p ^{2}G
	48,344.91	48,526.63	1.142	1.144	78.6 4d5s(^{1}D)5p ^{2}F	13.3 4d^2(^{1}D)5p ^{2}F
	57,741.16	57,747.69	1.240	1.143	82.2 4d5s(^{3}D)5p ^{2}F	8.8 4d^2(^{1}G)5p ^{2}F
9/2	29,839.87	29,856.52	1.164	1.174	98.2 4d^2(^{3}F)5p ^{4}G	1.4 4d^2(^{3}F)5p ^{4}F
	31,866.49	31,771.61	1.321	1.324	91.8 4d^2(^{3}F)5p ^{4}F	3.3 4d5s(^{3}D)5p ^{4}F
	35,185.64	35,179.51	1.109	1.118	77.1 4d^2(^{3}F)5p ^{2}G	18.5 4d^2(^{1}G)5p ^{2}G
	38,644.12	38,774.78	1.321	1.334	96.2 4d5s(^{3}D)5p ^{4}F	3.7 4d^2(^{3}F)5p ^{4}F
	40,878.25	40,918.70	1.083	1.021	44.5 4d^2(^{1}G)5p ^{2}H	40.9 4d^2(^{1}G)5p ^{2}G
	41,738.21	41,697.88	0.954	1.001	54.7 4d^2(^{1}G)5p ^{2}H	39.6 4d^2(^{1}G)5p ^{2}G
11/2	30,795.74	30,813.02	1.275	1.273	99.8 4d^2(^{3}F)5p ^{4}G	0.1 4d^2(^{1}G)5p ^{2}H
	42,409.93	42,287.84	1.080	1.091	99.9 4d^2(^{1}G)5p ^{2}H	0.1 4d^2(^{3}F)5p ^{4}G

Table 5
Zr II transition radial integrals obtained in the fitting procedure used in the oscillator strength parametrization method.

Transition	Value	Uncertainty
$<5p\|r^1\|5s>(4d^25p–4d^25s)$	−3.1522	0.02
$<5p\|r^1\|4d>(4d^25p–4d^3)$	1.7605	0.01
$<5p\|r^1\|6s>(4d^25p–4d^26s)$	−1.481	0.79
$<5p\|r^1\|5d>(4d^25p–4d^25d)$	2.289	0.01
$<4d\|r^1\|5p>(4d^25p–4d5p^2)$	1.584	0.01
$<5p\|r^1\|4d>(4d5s5p–4d^25s)$	1.408	0.01
$<5p\|r^1\|5s>(4d5s5p–4d5s^2)$	−2.995	0.02
$<5s\|r^1\|5p>(4d5s5p–4d5p^2)$	−7.88	0.04
$<5p\|r^1\|4d>(5s^25p–4d5s^2)$	1.267	0.01
$<6p\|r^1\|5s>(4d^26p–4d^25s)$	−0.03	0.02
$<6p\|r^1\|4d>(4d^26p–4d^3)$	0.25	0.01

Table 6
Optimized radial parameter values (in cm^{-1}) adopted in the HFR+CPOL model.

Configuration	Parameter	*Ab initio* value	Fitted value	Ratio
Even parity				
$4d^25s$	E_{av}	8394	8185	
	$F^2(4d,4d)$	48,301	36,089	0.747
	$F^4(4d,4d)$	31,255	23,579	0.754
	α		−13	
	β		345	
	ζ_{4d}	404	377	0.933
	$G^2(4d,5s)$	15,827	13,124	0.829
$4d5s^2$	E_{av}	17,393	16,265	
	ζ_{4d}	458	445	0.972
$4d^3$	E_{av}	13,048	12,076	
	$F^2(4d,4d)$	44,605	32,982	0.739
	$F^4(4d,4d)$	28,637	19,489	0.681
	α		3	
	β		354	
	ζ_{4d}	352	317	0.901
Odd parity				
$4d^25p$	E_{av}	36,627	37,497	
	$F^2(4d,4d)$	49,231	37,353	0.759
	$F^4(4d,4d)$	31,924	21,696	0.680
	α		40	
	β		−315	
	ζ_{4d}	415	390	0.940
	ζ_{5p}	620	874	1.410
	$F^2(4d,5p)$	17,387	13,394	0.770
	$G^1(4d,5p)$	9035	7392	0.818
	$G^3(4d,5p)$	6944	4784	0.689
4d5s5p	E_{av}	42,524	44,836	
	ζ_{4d}	467	432	0.925
	ζ_{5p}	776	834	1.075
	$F^2(4d,5p)$	18,831	17,090	0.908
	$G^2(4d,5s)$	15,417	11,695	0.759
	$G^1(4d,5p)$	9031	8672	0.960
	$G^3(4d,5p)$	7204	4857	0.674
	$G^1(5s,5p)$	34,180	24,825	0.726
$4d^25p$–4d5s5p	$R^2(4d4d,4d5s)$	−18,830	−13,797	0.733
	$R^2(4d5p,5s5p)$	−16,560	−12,133	0.733
	$R^1(4d5p,5s5p)$	−16,663	−12,209	0.733

help of Racah algebra and level eigenvectors. We then treat the radial integrals: $\int_0^\infty R_{nl}(r)rR_{n'l'}(r)dr$ as free parameters in the least squares fit to experimental oscillator strength values as in [20]. We give the main extracted values in Table 5. The values of the six remaining integrals are fixed to zero since they do not play any influent role in fitting procedure and then are subject inevitably to high uncertainties.

3. Pseudo-relativistic Hartree–Fock calculations

In order to assess the reliability of the results obtained with the oscillator strength parametrization approach, a second method was used for modelling the atomic structure and computing the radiative data in Zr II. This latter was the pseudo-relativistic Hartree–Fock (HFR) method, originally described by Cowan [18] and modified for taking core-polarization effects into account (HFR+CPOL, see e.g. [21,22]). For the present calculations, we adopted the same model as the one used in our previous study dedicated to the same ion [4]. The computational procedure included the following configurations: $4d5s^2$, $4d5p^2$, $4d5d^2$, $4d4f^2$, $4d5f^2$, 4d5s6s, 4d5s5d, 4d5s6d, 4d5p4f, 4d5p5f, $4d^25s$, $4d^26s$, $4d^25d$, $4d^26d$, $4d^3$, $5s^26s$, $5s^25d$, $5s^26d$ (even parity) and 4d5s5p, 4d5s6p, 4d5s4f, 4d5s5f, 4d5p5d, 4d5d4f, 4d5d5f, $4d^25p$, $4d^26p$, $4d^24f$, $4d^25f$, $5s^25p$, $5s^26p$, $5s^24f$, $5s^25f$ (odd parity). A Zr^{4+} ionic core of the type $1s^22s^22p^63s^23p^63d^{10}4s^24p^6$ was considered with a value for the dipole polarizability, α_d, equal to $2.98a_0^3$ [23] and a cut-off radius, $r_c=1.35a_0$, which corresponds to the HFR expectation value of $\langle r\rangle$ for the outermost core orbital (4p). In addition, the final wavefunctions were obtained by a parametric fit of the radial energy parameters using the experimental energy levels. More precisely, the 35 even-parity levels reported by Moore [12] as belonging to $4d5s^2$, $4d^25s$ and $4d^3$ were used to adjust the numerical values of the average energies (E_{av}), the electrostatic integrals (F^k, G^k) and the spin–orbit parameters (ζ_{nl}) together with the effective interaction parameters (α, β) corresponding to these three configurations. For the odd parity, the 68 experimental levels taken from the same compilation were used to optimize all the radial parameters, including the interaction configuration integrals (R^k), corresponding to the 4d5s5p and $4d^25p$ configurations. The standard deviations of the fitting process were found to be equal to 46 cm^{-1} for the even parity and 177 cm^{-1} for the odd parity. The numerical values of the radial parameters adopted in our HFR+CPOL calculations are given in Table 6. All the other electrostatic integrals (not adjusted in the semi-empirical process) were reduced to 80% of their *ab initio* values, as suggested by Cowan [18], while the spin–orbit parameters were kept to their *ab initio* values.

4. Results and discussion

The radiative lifetimes computed using our HFR+CPOL model for all the 68 experimentally known odd-parity energy levels in Zr II were already reported in a previous paper [4]. In the latter, it was shown that an overall good agreement, within about 15% on average, was reached when comparing our results to available experimental data, if we except the $y\ ^2F_{7/2}$ level at 37,787.59 cm^{-1}, the $z\ ^4P_{3/2}$ level at 38,133.50 cm^{-1}, the $x\ ^2P_{3/2}$ level at 45,568.21 cm^{-1} for which unexplained larger discrepancies (up to a factor of 3) were found. In view of this general good agreement, we can expect the calculated HFR+CPOL radiative transition rates to be accurate to within 15–20%

Table 7
Oscillator strengths for selected transitions (log *gf* (HFR+CPOL) < −1.0) in Zr II.

λ (Å)[a]	Lower level[b]			Upper level[b]			log *gf* (Exp)	log *gf* (this work)	
	E (cm⁻¹)		J	E (cm⁻¹)		J	[5]	OSP	HFR+CPOL
1878.440	4506	(e)	2.5	57,741	(o)	3.5			−0.24
1893.448	4248	(e)	1.5	57,062	(o)	2.5			−0.54
1902.714	4506	(e)	2.5	57,062	(o)	2.5			−0.93
1911.273	4248	(e)	1.5	56,569	(o)	2.5			−0.76
1920.715	4506	(e)	2.5	56,569	(o)	2.5			−0.27
1938.464	4248	(e)	1.5	55,836	(o)	1.5			−0.22
1948.177	4506	(e)	2.5	55,836	(o)	1.5			−0.62
1948.973	5753	(e)	2.5	57,062	(o)	2.5			−0.22
1950.323	6468	(e)	3.5	57,741	(o)	3.5			−0.31
1981.857	6112	(e)	1.5	56,569	(o)	2.5			−0.68
1995.935	6468	(e)	3.5	56,569	(o)	2.5			0.17
1996.701	5753	(e)	2.5	55,836	(o)	1.5			−0.07
2015.951	8153	(e)	4.5	57,741	(o)	3.5			−0.33
2030.865	7838	(e)	3.5	57,062	(o)	2.5			−0.45
2064.031	13,429	(e)	1.5	61,862	(o)	1.5			−0.91
2095.814	14,163	(e)	2.5	61,862	(o)	1.5			0.06
2109.659	13,429	(e)	1.5	60,815	(o)	0.5			−0.20
2121.186	14,733	(e)	2.5	61,862	(o)	1.5			−0.38
2137.673	6112	(e)	1.5	52,877	(o)	1.5			−0.82
2149.128	14,299	(e)	1.5	60,815	(o)	0.5			−0.71
2291.111	13,429	(e)	1.5	57,062	(o)	2.5			0.16
2294.015	14,163	(e)	2.5	57,741	(o)	3.5			0.50
2295.466	14,190	(e)	4.5	57,741	(o)	3.5			0.12
2317.272	13,429	(e)	1.5	56,569	(o)	2.5			−0.09
2324.446	14,733	(e)	2.5	57,741	(o)	3.5			−0.44
2324.746	14,060	(e)	3.5	57,062	(o)	2.5			0.08
2330.336	14,163	(e)	2.5	57,062	(o)	2.5			−0.10
2337.734	14,299	(e)	1.5	57,062	(o)	2.5			−0.97
2351.686	14,060	(e)	3.5	56,569	(o)	2.5			−0.86
2357.378	13,429	(e)	1.5	55,836	(o)	1.5			0.07
2357.406	14,163	(e)	2.5	56,569	(o)	2.5			0.07
2372.940	5753	(e)	2.5	47,882	(o)	2.5			−0.61
2387.201	6468	(e)	3.5	48,345	(o)	3.5			−0.60
2392.669	20,080	(e)	1.5	61,862	(o)	1.5			−0.27
2398.926	14,163	(e)	2.5	55,836	(o)	1.5			−0.95
2426.391	19,614	(e)	0.5	60,815	(o)	0.5			−0.60
2441.993	4248	(e)	1.5	45,186	(o)	2.5			−0.97
2449.844	4248	(e)	1.5	45,055	(o)	1.5			−0.14
2457.433	4506	(e)	2.5	45,186	(o)	2.5			0.02
2487.300	8153	(e)	4.5	48,345	(o)	3.5			−0.50
2496.491	7838	(e)	3.5	47,882	(o)	2.5			−0.73
2503.354	0	(e)	1.5	39,934	(o)	0.5			−0.10
2532.481	763	(e)	3.5	40,239	(o)	3.5	−0.69	−0.68	−0.60
2542.122	315	(e)	2.5	39,640	(o)	2.5	−0.64	−0.55	−0.46
2550.753	0	(e)	1.5	39,192	(o)	1.5	−0.64	−0.64	−0.54
2568.891	1323	(e)	4.5	40,239	(o)	3.5	0.32	0.32	0.39
2571.400	315	(e)	2.5	39,192	(o)	1.5	0.04	−0.01	0.10
2571.468	763	(e)	3.5	39,640	(o)	2.5	0.23	0.16	0.26
2583.410	4506	(e)	2.5	43,202	(o)	2.5			−0.83

Table 7 (*continued*)

λ (Å)[a]	Lower level[b]			Upper level[b]			log *gf* (Exp)	log *gf* (this work)	
	E (cm^{-1})		*J*	*E* (cm^{-1})		*J*	[5]	OSP	HFR+CPOL
2589.066	4248	(e)	1.5	42,861	(o)	2.5			−0.67
2609.647	19,433	(e)	3.5	57,741	(o)	3.5			−0.68
2630.891	4506	(e)	2.5	42,504	(o)	3.5			−0.42
2639.082	763	(e)	3.5	38,644	(o)	4.5	−0.67	−0.95	−0.77
2662.525	19,515	(e)	2.5	57,062	(o)	2.5			−0.86
2678.646	1323	(e)	4.5	38,644	(o)	4.5	0.28	0.08	0.25
2681.747	763	(e)	3.5	38,041	(o)	3.5		−0.79	−0.50
2691.991	19,433	(e)	3.5	56,569	(o)	2.5			−0.32
2692.594	8058	(e)	2.5	45,186	(o)	2.5			−0.80
2693.522	315	(e)	2.5	37,430	(o)	3.5	−0.98	−1.21	−0.75
2694.052	5753	(e)	2.5	42,861	(o)	2.5			−0.67
2699.593	315	(e)	2.5	37,346	(o)	2.5	−1.17	−0.83	−0.61
2700.139	763	(e)	3.5	37,788	(o)	3.5	−0.08	−0.36	−0.76
2711.502	0	(e)	1.5	36,869	(o)	2.5	−0.80	−1.12	−0.94
2712.418	315	(e)	2.5	37,171	(o)	2.5	−0.99	−0.90	−0.49
2722.610	1323	(e)	4.5	38,041	(o)	3.5	0.06	−0.60	−0.46
2726.491	763	(e)	3.5	37,430	(o)	3.5	−0.22	−0.50	−0.04
2726.937	25,202	(e)	0.5	61,862	(o)	1.5			−0.25
2728.561	0	(e)	1.5	36,639	(o)	1.5		−0.65	−0.73
2734.845	315	(e)	2.5	36,869	(o)	2.5	−0.06	−0.43	−0.35
2739.731	20,080	(e)	1.5	56,569	(o)	2.5			−0.58
2741.569	1323	(e)	4.5	37,788	(o)	3.5	−0.90	−0.51	−0.23
2742.538	0	(e)	1.5	36,452	(o)	1.5	−0.14	−0.59	−0.24
2745.854	763	(e)	3.5	37,171	(o)	2.5	−0.31	−0.45	−0.60
2752.200	315	(e)	2.5	36,639	(o)	1.5	−0.15	−1.13	−0.46
2752.438	19,515	(e)	2.5	55,836	(o)	1.5			−0.44
2758.792	0	(e)	1.5	36,237	(o)	0.5	−0.56	−0.91	−0.58
2759.938	19,614	(e)	0.5	55,836	(o)	1.5			−0.83
2766.421	315	(e)	2.5	36,452	(o)	1.5		−0.74	−0.75
2768.740	1323	(e)	4.5	37,430	(o)	3.5	−0.93	−1.35	−0.42
2768.839	763	(e)	3.5	36,869	(o)	2.5		−2.29	−0.31
2774.145	6468	(e)	3.5	42,504	(o)	3.5			−0.57
2796.899	5724	(e)	0.5	41,468	(o)	1.5			−0.66
2799.135	5753	(e)	2.5	41,468	(o)	1.5			−0.94
2807.142	25,202	(e)	0.5	60,815	(o)	0.5			−0.73
2810.916	6112	(e)	1.5	41,677	(o)	2.5			−0.41
2818.738	7736	(e)	1.5	43,202	(o)	2.5			−0.06
2825.555	7513	(e)	0.5	42,894	(o)	1.5			−0.07
2833.909	7513	(e)	0.5	42,789	(o)	0.5			−0.79
2839.331	6468	(e)	3.5	41,677	(o)	2.5			−0.78
2843.506	7736	(e)	1.5	42,894	(o)	1.5			−0.53
2844.576	8058	(e)	2.5	43,202	(o)	2.5			0.29
2848.180	5753	(e)	2.5	40,853	(o)	3.5			−0.61
2851.967	7736	(e)	1.5	42,789	(o)	0.5			−0.08
2869.802	8058	(e)	2.5	42,894	(o)	1.5			−0.08
2883.794	7838	(e)	3.5	42,504	(o)	3.5			−0.94
2901.623	13,429	(e)	1.5	47,882	(o)	2.5			−0.60
2905.227	6468	(e)	3.5	40,878	(o)	4.5			−0.59
2910.245	8153	(e)	4.5	42,504	(o)	3.5			−0.93
2915.973	3758	(e)	4.5	38,041	(o)	3.5	−0.50	−0.80	−0.29

2918.246	8153	(e)	4.5	42,410	(o)	5.5			−0.10
2924.660	14,163	(e)	2.5	48,345	(o)	3.5			−0.66
2927.019	14,190	(e)	4.5	48,345	(o)	3.5			0.45
2936.286	3300	(e)	3.5	37,346	(o)	2.5	−0.88	−1.20	−0.99
2937.730	3758	(e)	4.5	37,788	(o)	3.5		−0.81	−0.65
2948.950	7838	(e)	3.5	41,738	(o)	4.5			−0.26
2951.465	3300	(e)	3.5	37,171	(o)	2.5	−0.77	−0.71	−0.40
2955.781	14,060	(e)	3.5	47,882	(o)	2.5			0.31
2962.673	2895	(e)	2.5	36,639	(o)	1.5	−0.57	−0.60	−0.46
2969.592	2572	(e)	1.5	36,237	(o)	0.5	−0.70	−0.74	−0.66
2976.614	8153	(e)	4.5	41,738	(o)	4.5			−0.39
2981.001	4506	(e)	2.5	38,041	(o)	3.5	−0.80	−0.39	−0.48
3003.743	4506	(e)	2.5	37,788	(o)	3.5	−0.55	−1.52	−0.39
3005.444	19,614	(e)	0.5	52,877	(o)	1.5			−0.96
3020.450	4248	(e)	1.5	37,346	(o)	2.5	−0.56	−0.47	−0.48
3028.045	7838	(e)	3.5	40,853	(o)	3.5			−0.01
3036.514	4248	(e)	1.5	37,171	(o)	2.5	−0.96	−2.53	−0.95
3048.219	20,080	(e)	1.5	52,877	(o)	1.5			−0.53
3054.837	8153	(e)	4.5	40,878	(o)	4.5			0.08
3057.221	8153	(e)	4.5	40,853	(o)	3.5			−0.93
3083.458	7513	(e)	0.5	39,934	(o)	0.5			−0.47
3095.073	315	(e)	2.5	32,615	(o)	2.5	−0.84	−0.61	−0.72
3099.231	0	(e)	1.5	32,257	(o)	1.5	−0.96	−0.73	−0.85
3106.581	8058	(e)	2.5	40,239	(o)	3.5	0.09	0.14	0.27
3110.871	763	(e)	3.5	32,899	(o)	3.5	−0.90	−0.64	−0.68
3125.926	0	(e)	1.5	31,981	(o)	0.5	−0.70	−0.50	−0.60
3129.153	4248	(e)	1.5	36,197	(o)	0.5			−0.23
3129.763	315	(e)	2.5	32,257	(o)	1.5	−0.54	−0.39	−0.49
3133.489	7736	(e)	1.5	39,640	(o)	2.5	−0.19	−0.08	0.00
3138.683	763	(e)	3.5	32,615	(o)	2.5	−0.37	−0.23	−0.34
3155.684	7513	(e)	0.5	39,192	(o)	1.5	−0.57	−0.44	−0.38
3156.996	4248	(e)	1.5	35,915	(o)	1.5	−0.93	−0.88	−0.83
3164.303	5753	(e)	2.5	37,346	(o)	2.5	−0.33	−0.24	−0.21
3165.452	8058	(e)	2.5	39,640	(o)	2.5	−0.69	−0.87	-0.59
3165.991	1323	(e)	4.5	32,899	(o)	3.5	−0.13	0.01	−0.09
3166.258	6468	(e)	3.5	38,041	(o)	3.5	−0.51	−0.21	−0.39
3178.091	7736	(e)	1.5	39,192	(o)	1.5	−0.62	−0.61	−0.46
3181.938	5753	(e)	2.5	37,171	(o)	2.5	−0.75	−2.32	−0.64
3182.849	4506	(e)	2.5	35,915	(o)	1.5	0.01	0.07	0.13
3191.927	6468	(e)	3.5	37,788	(o)	3.5	−0.52	−2.00	−0.17
3214.190	763	(e)	3.5	31,866	(o)	4.5	−0.40	−0.38	−0.30
3231.692	315	(e)	2.5	31,249	(o)	3.5	−0.47	−0.42	−0.33
3236.631	14,299	(e)	1.5	45,186	(o)	2.5			−0.91
3241.042	315	(e)	2.5	31,160	(o)	2.5	−0.57		−0.64
3242.149	14,733	(e)	2.5	45,568	(o)	1.5			−0.88
3250.436	14,299	(e)	1.5	45,055	(o)	1.5			−0.04
3264.809	7513	(e)	0.5	38,134	(o)	1.5	−1.21	−0.57	−0.55
3271.123	4248	(e)	1.5	34,810	(o)	0.5			−0.89
3272.221	0	(e)	1.5	30,551	(o)	2.5			−0.49
3273.067	1323	(e)	4.5	31,866	(o)	4.5	0.30	0.33	0.35
3279.266	763	(e)	3.5	31,249	(o)	3.5	0.12	0.10	0.13
3282.837	14,733	(e)	2.5	45,186	(o)	2.5			0.17
3284.703	0	(e)	1.5	30,435	(o)	1.5	−0.37	−0.45	−0.41
3285.773	11,984	(e)	4.5	42,410	(o)	5.5			−0.71
3285.880	8058	(e)	2.5	38,483	(o)	2.5			−0.47
3288.799	7736	(e)	1.5	38,134	(o)	1.5	−0.38	−0.42	−0.29
3296.401	7736	(e)	1.5	38,063	(o)	0.5			−0.87

Table 7 (*continued*)

λ (Å)[a]	Lower level[b]			Upper level[b]			log *gf* (Exp)	log *gf* (this work)	
	E (cm^{-1})		J	E (cm^{-1})		J	[5]	OSP	HFR+CPOL
3302.661	9969	(e)	2.5	40,239	(o)	3.5	−1.01	−1.33	−0.78
3305.153	315	(e)	2.5	30,562	(o)	3.5	−0.65	−0.82	−0.76
3306.275	315	(e)	2.5	30,551	(o)	2.5			−0.17
3314.488	5753	(e)	2.5	35,915	(o)	1.5	−0.79	−0.71	−0.63
3322.974	6112	(e)	1.5	36,197	(o)	0.5			−0.54
3324.027	8058	(e)	2.5	38,134	(o)	1.5		−2.41	−0.64
3326.800	12,360	(e)	5.5	42,410	(o)	5.5			−0.03
3334.228	8058	(e)	2.5	38,041	(o)	3.5	−0.35	−0.50	−0.22
3334.607	4506	(e)	2.5	34,485	(o)	3.5	−0.69	−0.78	−0.66
3337.955	7838	(e)	3.5	37,788	(o)	3.5	−1.54	−5.13	−0.92
3340.574	1323	(e)	4.5	31,249	(o)	3.5	−0.57	−0.47	−0.45
3344.785	8153	(e)	4.5	38,041	(o)	3.5	−0.35	−0.10	−0.37
3354.390	6112	(e)	1.5	35,915	(o)	1.5	−0.92	−0.83	−0.71
3356.087	763	(e)	3.5	30,551	(o)	2.5			−0.39
3357.264	0	(e)	1.5	29,778	(o)	1.5	−0.66	−0.50	−0.48
3359.955	11,984	(e)	4.5	41,738	(o)	4.5			−0.28
3362.704	8058	(e)	2.5	37,788	(o)	3.5	−1.04	−0.43	−0.51
3373.443	8153	(e)	4.5	37,788	(o)	3.5	−0.44	−2.29	−0.02
3374.719	8058	(e)	2.5	37,682	(o)	1.5	−0.19	−0.11	−0.19
3387.873	7838	(e)	3.5	37,346	(o)	2.5	−0.14	−0.09	−0.02
3388.287	0	(e)	1.5	29,505	(o)	2.5	−0.41	−0.62	−0.53
3391.982	1323	(e)	4.5	30,796	(o)	5.5	0.57	0.56	0.61
3393.122	315	(e)	2.5	29,778	(o)	1.5	−0.74	−0.63	−0.61
3396.318	7736	(e)	1.5	37,171	(o)	2.5	−0.63	−0.49	−0.43
3396.662	13,429	(e)	1.5	42,861	(o)	2.5			−0.35
3399.339	2572	(e)	1.5	31,981	(o)	0.5	−0.72	−0.64	−0.64
3402.867	12,360	(e)	5.5	41,738	(o)	4.5			0.00
3403.673	8058	(e)	2.5	37,430	(o)	3.5	−0.60	−0.32	−0.89
3404.825	2895	(e)	2.5	32,257	(o)	1.5	−0.49	−0.40	−0.39
3408.096	7838	(e)	3.5	37,171	(o)	2.5	−0.66	−3.32	−0.52
3410.236	3300	(e)	3.5	32,615	(o)	2.5	−0.31	−0.22	−0.22
3430.513	3758	(e)	4.5	32,899	(o)	3.5	−0.16	−0.05	−0.04
3431.552	7736	(e)	1.5	36,869	(o)	2.5	−0.95	−0.70	−0.95
3432.394	7513	(e)	0.5	36,639	(o)	1.5	−0.72	−0.70	−0.64
3433.900	8058	(e)	2.5	37,171	(o)	2.5	−0.89	−0.72	−0.72
3437.136	5724	(e)	0.5	34,810	(o)	0.5			−0.41
3438.226	763	(e)	3.5	29,840	(o)	4.5	0.41	0.40	0.45
3457.548	4506	(e)	2.5	33,419	(o)	2.5			−0.41
3458.920	7736	(e)	1.5	36,639	(o)	1.5	−0.48	−0.54	−0.45
3459.960	11,984	(e)	4.5	40,878	(o)	4.5			−0.76
3463.018	11,984	(e)	4.5	40,853	(o)	3.5			0.38
3471.112	14,060	(e)	3.5	42,861	(o)	2.5			−0.44
3478.495	9743	(e)	1.5	38,483	(o)	2.5			−0.85
3479.028	4248	(e)	1.5	32,984	(o)	1.5	−0.67	−0.75	−0.61
3479.383	5753	(e)	2.5	34,485	(o)	3.5	0.18	0.12	0.22
3480.368	7513	(e)	0.5	36,237	(o)	0.5	−0.78	−0.65	−0.64
3481.136	6468	(e)	3.5	35,186	(o)	4.5			0.34
3483.526	6112	(e)	1.5	34,810	(o)	0.5			−0.37
3496.191	315	(e)	2.5	28,909	(o)	3.5	0.26	0.24	0.29
3505.482	12,360	(e)	5.5	40,878	(o)	4.5			0.28

3505.682	1323	(e)	4.5	29,840	(o)	4.5	−0.39	−0.39	−0.31
3506.047	9969	(e)	2.5	38,483	(o)	2.5			−0.68
3514.631	14,060	(e)	3.5	42,504	(o)	3.5			−0.82
3521.273	9743	(e)	1.5	38,134	(o)	1.5	−1.39	−1.41	−0.79
3525.803	2895	(e)	2.5	31,249	(o)	3.5	−0.96	−0.86	−0.83
3527.422	14,163	(e)	2.5	42,504	(o)	3.5			−0.17
3529.989	9743	(e)	1.5	38,063	(o)	0.5			−0.96
3530.855	14,190	(e)	4.5	42,504	(o)	3.5			−0.34
3542.639	14,190	(e)	4.5	42,410	(o)	5.5			0.44
3549.511	9969	(e)	2.5	38,134	(o)	1.5	−0.72	−0.35	−0.21
3551.938	763	(e)	3.5	28,909	(o)	3.5	−0.36	−0.35	−0.29
3554.079	9553	(e)	0.5	37,682	(o)	1.5	−0.81	−0.57	−0.57
3556.585	3758	(e)	4.5	31,866	(o)	4.5	0.07	0.13	0.17
3565.415	13,429	(e)	1.5	41,468	(o)	1.5			−0.58
3572.472	0	(e)	1.5	27,984	(o)	2.5	0.03	0.06	0.10
3573.054	2572	(e)	1.5	30,551	(o)	2.5			−0.91
3576.842	3300	(e)	3.5	31,249	(o)	3.5	−0.12	−0.02	0.03
3578.211	9743	(e)	1.5	37,682	(o)	1.5	−0.66	−0.49	−0.65
3587.943	2572	(e)	1.5	30,435	(o)	1.5	−0.80	−0.98	−0.96
3611.889	14,060	(e)	3.5	41,738	(o)	4.5			0.27
3612.309	25,202	(e)	0.5	52,877	(o)	1.5			−0.09
3613.102	315	(e)	2.5	27,984	(o)	2.5	−0.58	−0.57	−0.51
3614.765	2895	(e)	2.5	30,551	(o)	2.5			−0.14
3629.025	14,190	(e)	4.5	41,738	(o)	4.5			−0.80
3633.488	14,163	(e)	2.5	41,677	(o)	2.5			−0.55
3650.697	25,202	(e)	0.5	52,586	(o)	0.5			−0.31
3662.127	13,429	(e)	1.5	40,727	(o)	0.5			−0.45
3671.265	5753	(e)	2.5	32,984	(o)	1.5	−0.58	−0.43	−0.52
3674.696	2572	(e)	1.5	29,778	(o)	1.5	−0.51	−0.39	−0.33
3678.878	14,163	(e)	2.5	41,337	(o)	1.5			−0.16
3679.607	14,299	(e)	1.5	41,468	(o)	1.5			−0.83
3697.435	3758	(e)	4.5	30,796	(o)	5.5	−0.78	−0.71	−0.65
3698.152	8153	(e)	4.5	35,186	(o)	4.5			0.25
3709.266	6468	(e)	3.5	33,419	(o)	2.5			−0.16
3710.421	14,733	(e)	2.5	41,677	(o)	2.5			−0.72
3714.794	4248	(e)	1.5	31,160	(o)	2.5	−0.96		−0.93
3727.711	14,060	(e)	3.5	40,878	(o)	4.5			−0.28
3731.260	14,060	(e)	3.5	40,853	(o)	3.5			0.01
3745.966	14,190	(e)	4.5	40,878	(o)	4.5			0.12
3751.606	7838	(e)	3.5	34,485	(o)	3.5	0.00	0.02	0.10
3766.795	3300	(e)	3.5	29,840	(o)	4.5	−0.83	−0.77	−0.70
3796.493	8153	(e)	4.5	34,485	(o)	3.5	−0.89	−0.85	-0.74
3817.593	4248	(e)	1.5	30,435	(o)	1.5	−1.13	−0.91	−0.80
3836.762	4506	(e)	2.5	30,562	(o)	3.5	−0.12	−0.10	−0.03
3842.995	2895	(e)	2.5	28,909	(o)	3.5	−0.94	−0.89	−0.81
3881.971	19,433	(e)	3.5	45,186	(o)	2.5			−0.47
3914.313	19515	(e)	2.5	45,055	(o)	1.5			−0.52
3915.959	4248	(e)	1.5	29,778	(o)	1.5	−0.85	−1.12	−0.92
3929.499	19,614	(e)	0.5	45,055	(o)	1.5			−0.91
3934.094	2572	(e)	1.5	27,984	(o)	2.5	−1.08	−1.03	−0.95
3934.791	5753	(e)	2.5	31,160	(o)	2.5	−0.91		−0.81
3958.230	4248	(e)	1.5	29,505	(o)	2.5	−0.32	−0.30	−0.22
3982.025	20,080	(e)	1.5	45,186	(o)	2.5			−0.84
3991.152	6112	(e)	1.5	31,160	(o)	2.5	−0.31		−0.18
3998.954	4506	(e)	2.5	29,505	(o)	2.5	−0.52	−0.49	−0.40
4024.417	8058	(e)	2.5	32,899	(o)	3.5	−1.13	−1.16	−0.92
4029.684	5753	(e)	2.5	30,562	(o)	3.5	−0.78	−0.77	−0.68

Table 7 (*continued*)

λ (Å)[a]	Lower level[b]			Upper level[b]			log *gf* (Exp)	log *gf* (this work)	
	E (cm^{-1})		*J*	*E* (cm^{-1})		*J*	[5]	OSP	HFR+CPOL
4045.638	5724	(e)	0.5	30,435	(o)	1.5	−0.86	−0.71	−0.60
4048.680	6468	(e)	3.5	31,160	(o)	2.5	−0.53		−0.43
4050.316	5753	(e)	2.5	30,435	(o)	1.5	−1.06	−0.86	−0.74
4149.217	6468	(e)	3.5	30,562	(o)	3.5	−0.04	−0.03	0.06
4156.276	5724	(e)	0.5	29,778	(o)	1.5	−0.78	−0.97	−0.86
4161.213	5753	(e)	2.5	29,778	(o)	1.5	−0.59	−0.69	−0.62
4179.807	13,429	(e)	1.5	37,346	(o)	2.5	−0.68	−0.92	−0.84
4191.508	14,190	(e)	4.5	38,041	(o)	3.5	−1.07	−0.82	−0.90
4208.977	5753	(e)	2.5	29,505	(o)	2.5	−0.51	−0.49	−0.42
4231.668	14,163	(e)	2.5	37,788	(o)	3.5	−0.79	−2.51	−0.74
4236.609	14,190	(e)	4.5	37,788	(o)	3.5		−2.39	−0.57
4282.206	19,515	(e)	2.5	42,861	(o)	2.5			−0.43
4289.143	14,733	(e)	2.5	38,041	(o)	3.5	−1.68	−0.88	−0.80
4293.116	14,060	(e)	3.5	37,346	(o)	2.5	−1.01	−1.08	−0.77
4333.252	19,433	(e)	3.5	42,504	(o)	3.5			−0.32
4336.381	14,733	(e)	2.5	37,788	(o)	3.5	−1.75	−3.05	−0.42
4337.614	14,299	(e)	1.5	37,346	(o)	2.5	−1.22	−0.92	−0.54
4359.720	9969	(e)	2.5	32,899	(o)	3.5	−0.51	−0.36	−0.30
4370.819	14,299	(e)	1.5	37,171	(o)	2.5		−3.84	−0.99
4370.947	9743	(e)	1.5	32,615	(o)	2.5	−0.77	−0.67	−0.60
4379.742	12,360	(e)	5.5	35,186	(o)	4.5			−0.19
4414.539	9969	(e)	2.5	32,615	(o)	2.5	−1.08	−1.00	−0.95
4440.452	9743	(e)	1.5	32,257	(o)	1.5	−1.04	−0.94	−0.89
4443.007	11,984	(e)	4.5	34,485	(o)	3.5	−0.42	−0.56	−0.31
4482.048	19,433	(e)	3.5	41,738	(o)	4.5			−0.98
4494.418	19,433	(e)	3.5	41,677	(o)	2.5			−0.18
4496.980	5753	(e)	2.5	27,984	(o)	2.5	−0.89	−0.97	−0.84
4553.934	19,515	(e)	2.5	41,468	(o)	1.5			−0.40
4574.502	19,614	(e)	0.5	41,468	(o)	1.5			−0.74
4601.953	19,614	(e)	0.5	41,337	(o)	1.5			−0.89
4629.079	20,080	(e)	1.5	41,677	(o)	2.5			−0.35
4661.784	19,433	(e)	3.5	40,878	(o)	4.5			−0.58
4685.185	19,515	(e)	2.5	40,853	(o)	3.5			−0.53
4703.003	20,080	(e)	1.5	41,337	(o)	1.5			−0.60
5350.089	14,733	(e)	2.5	33,419	(o)	2.5			−0.33
5350.373	14,299	(e)	1.5	32,984	(o)	1.5	−1.16	−0.78	−0.57

[a] The wavelengths, given in vacuum (air) below (above) 2000 Å are deduced from the experimental energy level values.
[b] Experimental energy levels taken from [12].

at least for most of the strongest lines. In Table 7, we give the oscillator strengths computed in the present work using both methods described in Sections 2 and 3 for a sample of about 300 selected Zr II transitions in the spectral region from 1878 to 5350 Å. More precisely, only lines with HFR+CPOL log *gf*-values greater than −1.0 are reported in this table in which are also given the available numerical values deduced from experimental measurements [5]. A more comprehensive table containing the radiative parameters for 1329 Zr II lines covering the wavelength range 1616–14,746 Å is available as Supplementary file.

When looking at Table 7, we can notice that oscillator strengths computed with both methods used in the present work agree generally within 30% although much larger discrepancies (up to several orders of magnitude) are observed for some lines, such as those appearing e.g. at 3003.743, 3036.514, 3181.938, 3191.927, 3337.955, 3373.443, 3408.096, 4231.668, 4236.609 and 4336.381 Å. However, for these transitions, although non-negligible discrepancies subsist, our HFR+CPOL results tend toward better agreement with the available experimental *gf*-values than those obtained with the oscillator strength parametrization approach. This is confirmed by the quite good agreement between the HFR+CPOL lifetimes and laser spectroscopy measurements previously reported [4] for the odd-parity levels involved in the corresponding transitions, i.e. those situated at 37,171 cm^{-1} ($J=5/2$) and 37,788 cm^{-1} ($J=7/2$).

The comparison between oscillator strengths calculated in the present work using our two semi-empirical approaches is illustrated in Fig. 1 for Zr II transitions with log $gf < -2.0$. It is not worth making the comparison for weaker transitions since most of them were found to be affected by large cancellation effects in the HFR+CPOL line strength calculations, indicating that those results could be affected by large uncertainties. It is clear from this figure that, if a satisfactory agreement between both sets of results is found for a large number of lines, rather large discrepancies subsist in several cases, in particular for weak transitions characterized by log *gf*-values smaller than −1.0. Each set of our semi-empirical results is separately compared with available experimental data in Figs. 2 and 3. When looking at those figures, it is found that both the oscillator strength parametrization and the pseudo-relativistic Hartree–Fock methods lead to radiative rates of the same order of accuracy for an atomic system so complex as that of singly ionized zirconium.

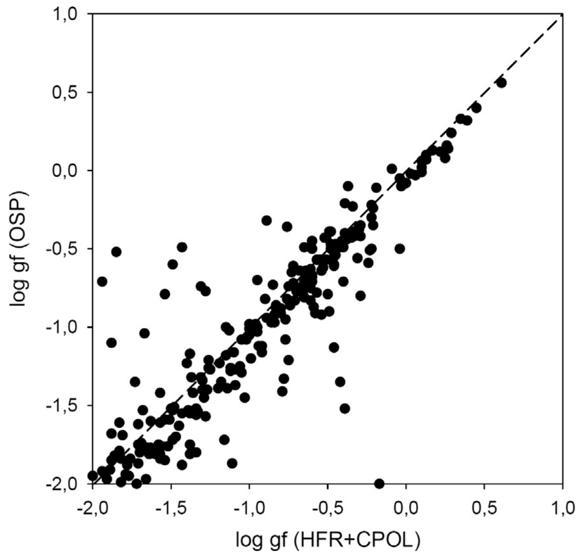

Fig. 1. Comparison between the log *gf*-values obtained in the present work with the oscillator strength parametrization method (OSP) and the pseudo-relativistic Hartree–Fock approach including core-polarization effects (HFR+CPOL). Only transitions with log $gf < -2$ are shown in the figure.

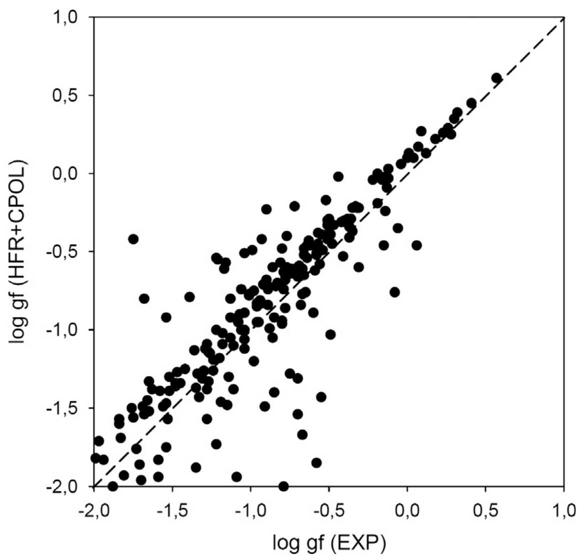

Fig. 2. Comparison between the log *gf*-values obtained in the present work with the pseudo-relativistic Hartree–Fock approach including core-polarization effects (HFR+CPOL) and the available experimental data [5]. Only transitions with log $gf < -2$ are shown in the figure.

5. Conclusion

Advances in the measurement of oscillator strengths are due both to the introduction of new techniques—in particular, fast-beam and laser spectroscopy—and to the technological improvement of the classical methods: a large number of astrophysically important transition probabilities have in fact been determined and moreover a notable improvement in precision has been brought; consequently the first measurements of solar abundance of most iron-group elements had been revised. Theoretically a large number of methods arised from investigations of the structure of stellar atmospheres based on reliable laboratory transition probabilities. We propose in this work two semi-empirical ways to express the strengths of Zr II optical transitions and to compare obtained data. A good agreement is observed between results obtained by these two approaches since one can see really bisecting line plots in Figs. 1–3. Furthermore these two methods confirm the well-founded basis of experimental data found in literature [5].

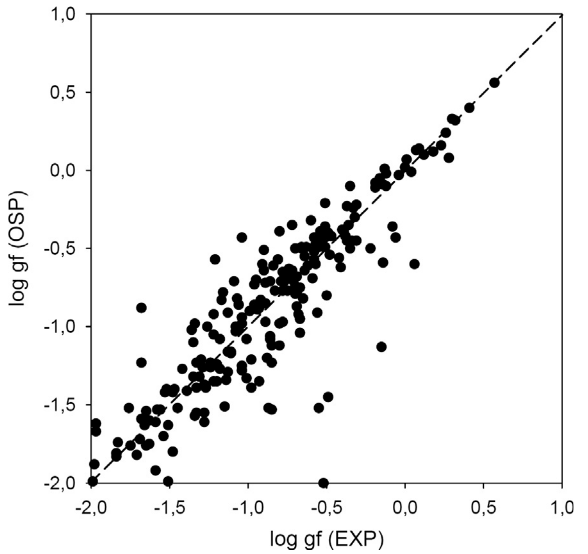

Fig. 3. Comparison between the log *gf*-values obtained in the present work with the oscillator strength parametrization method (OSP) and the available experimental data [5]. Only transitions with $\log gf < -2$ are shown in the figure.

Acknowledgments

PP and PQ are, respectively, Research Director and Research Associate of the Belgian Fund for Scientific Research F.R.S.-FNRS. Financial support from this organization is gratefully acknowledged (Grant n° FC 49142). SB deeply thanks Dr. J. Ruczkowski and Dr. M. Elantkowska for providing program package for oscillator strength parametrization.

Appendix A. Supporting information

Supplementary data associated with this article can be found in the online version at http://dx.doi.org/10.1016/j.jqsrt.2015.06.011.

References

[1] Bouazza S, Hannaford P, Wilson M. Fine structure of the odd-parity Rydberg series of Zr I. J Phys B 2003;36:1537 and references therein.
[2] Corliss CH, Bozman WR. Experimental transition probabilities for spectral lines of seventy elements; derived from the NBS Tables of spectral-lines intensities. (NBS Monograph). US Department of Commerce, National bureau of Standards: Washington.
[3] Biémont E, Grevesse N, Hannaford P, Lowe RM. Oscillator strengths for Zr I and Zr II and a new determination of the solar abundance of zirconium. Astrophys J 1981;248:867.
[4] Malcheva G, Blagoev K, Mayo R, Ortiz M, Xu HL, Svanberg S, et al. Radiative lifetimes and transition probabilities of astrophysical interest in Zr II. Mon Not R Astron Soc 2006;367:754–62.
[5] Ljung G, Nilsson H, Asplund M, Johansson S. New and improved experimental oscillator strengths in Zr II and the solar abundance of zirconium. Astron Astrophys 2006;456:1181.
[6] Bogdanovich P, Tautvaisiene G, Rudzikas Z, Momkauskaite A. A simple method of accounting for correlation effects in electron transitions and its application in finding oscillator strengths and the solar abundance of zirconium. Mon Not R Astron Soc 1995;280:95.
[7] Adelman S. Line identifications, elemental abundances, and equivalent widths for 21 sharp lined cool peculiar A stars and two comparison standards. Astrophys J 1973;26:1.
[8] Sadakane K. Spectroscopic study of the Ap star 73 Draconis - A model atmosphere analysis. Publ Astron Soc Jpn 1976;28:469.
[9] Kodaira K, Takada M. Differential curve-of-growth analyses of Mn–Hg stars II. Analyses of 53 Aur, HR 6997, and 112 Her, and final summary. Ann Tokyo Astron Obs, Second Ser 1978;17:79.
[10] Sikström CM, Lundberg H, Wahlgren GM, Li ZS, Lyngå C, Johansson S, et al. New Zr II oscillator strengths and the zirconium conflict in the HgMn star χLupi. Astron Astrophys 1999;343:297.
[11] Kiess CC, Kiess HK. Lines, terms and Zeeman effect. NBS J Res 1931;6:621.
[12] Moore CE. Atomic energy levels NBS circular. Washington, DC: US Government Printing office; 1971.
[13] Meggers WF, Corliss CH, Scribner BD. Tables of spectral-line intensities, Part 1. NBS 1975;145:1.
[14] Bouazza S. Semi-empirical hyperfine structure and ab-initio isotope shift prédictions in Zr II. Int J Quant Chem 2011;111:3000.
[15] Bouazza S, Quinet P, Palmeri P. Semi-empirical studies of atomic transition probabilities, oscillator strengths and radiative lifetimes in Hf II. J Quant Spectrosc Radiat Transf 2015;163:39.
[16] Ruczkowski J, Elantkowska M, Dembczynski J. An alternative method for determination of oscillator strengths. The example of Sc II. J Quant Spectrosc Radiat Transf 2014;145:20.
[17] Sobelman II. Atomic spectra and radiative transitions. Berlin: Springer-Verlag; 1978.
[18] Cowan RD. The theory of atomic structure and spectra. *Berkeley*: Berkeley University of California Press; 1981.
[19] Kurucz RL. Semiempirical calculation of gf values: Sc II ($3d+4s^2$)–($3d+4s$)4p. ⟨http://adsabs.harvard.edu/abs/1973SAOSR.351...K⟩.
[20] Ruczkowski J, Elantkowska M, Dembczynski J. Semi-empirical calculations of oscillator strengths and hyperfine structure for Ti II. J Quant Spectrosc Radiat Transf 2014;149:168.
[21] Quinet P, Palmeri P, Biémont E, McCurdy MM, Rieger G, Pinnington EH, et al. Experimental and theoretical lifetimes, branching fractions and oscillator strengths in LuII. Mon Not R Astron Soc 1999;307:934.
[22] Quinet P, Palmeri P, Biémont E, Li ZS, Zhang ZG, Svanberg S. Radiative lifetime measurements and transition probability calculations in lanthanide ions. J Alloys Compd 2002;344:255.
[23] Johnson WR, Kolb D, Huang KN. Electric-dipole, quadrupole, and magnetic-dipole susceptibilities and shielding factors for closed-shell ions of the He, Ne, Ar, Ni(Cu^+), Kr, Pb, and Xe isoelectronic sequences. At Data Nucl Data Tables 1983;28:333.